Solid State Ionics 67 (1994) 17–23
North-Holland

SOLID STATE IONICS

Polycrystalline, glassy and thin films of $LiMn_2O_4$

Chen Liquan [1] and Joop Schoonman
Laboratory for Inorganic Chemistry, Delft University of Technology, Julianalaan 136, 2628 BL Delft, The Netherlands

Received 13 October 1992; accepted for publication 12 October 1993

The influence of sintering temperature on the formation, phase purity, and electrical conductivity of $LiMn_2O_4$ has been investigated by means of X-ray diffraction and ac impedance analysis. Higher sintering temperatures lead to increased unit cell constants, more perfect lattices and a higher bulk electrical conductivity. Samples sintered at lower temperatures exhibit higher chemical diffusion coefficients for lithium. Attempts to prepare glassy $LiMn_2O_4$–B_2O_3 have been made. The conduction behaviour of the glass during the crystallization process has been studied. Polycrystalline thin films of $LiMn_2O_4$ have been prepared using electron beam evaporation. The temperature dependence of the electrical conductivity of the thin film did not differ substantially from that of bulk material, while the chemical diffusion coefficient for lithium is four orders of magnitude lower than that of samples sintered at 1100°C.

1. Introduction

Remarkable progress has been achieved in recent years in developing rechargeable Li/manganese oxides batteries. Among the lithium containing manganese oxides the spinel type compound $Li_{1+x}Mn_2O_4$ has attracted widespread attention [1,2]. In the structure the Mn_2O_4 framework remains intact during lithium insertion and extraction over the range $-1<x<1$ [3–6]. Lithium insertion into the lattice reduces the crystal symmetry from cubic for $LiMn_2O_4$ to tetragonal for $Li_{1+x}Mn_2O_4$ ($0.1<x<1.0$) due to the Jahn–Teller distortion caused by the increased Mn^{3+} concentration [3,6]. As a result a two-phase region with open circuit voltage 2.9 V exists over a wide range of compositions [7].

Recently, both Sony [8,9] and Moli Energy [10] have announced to produce rechargeable lithium batteries based on a lithium containing manganese oxide. The combination of high energy density (125 Wh/Kg) and power density (discharge rates C/2.5 h) with good cycle life (1000 cycles) marks a breakthrough in rechargeable lithium battery technology.

The cathode material used in such a battery is heat treated $LiOH \cdot MnO_2$, which is a composite containing lithium and manganese oxide [11]. With increasing temperature the spinel phase $LiMn_2O_4$ will be formed. A more recent paper has claimed that $LiMn_2O_4$ is not suitable for lithium rechargeable applications, because almost one half of the initial capacity of the battery will be lost at the second discharge [12].

The behaviour of the lithium containing manganese oxide cathodes is rather complicated, and it is necessary to obtain more insight into the relations between synthesis, structure, microstructure, defect structure and properties. In the first part of the present paper the effect of sintering temperature on the formation, phase purity, and electrical conductivity of $LiMn_2O_4$, as well as the chemical diffusion coefficient for lithium will be reported.

One effective way to improve the rechargeability of a cathode is to vary the metal–oxygen bond lengths in the structure through the use of network former B_2O_3 or P_2O_5 [13]. In the second part of the present paper the results for the first attempt to prepare glassy materials in the system $LiMn_2O_4 \cdot B_2O_3$ will be presented.

Following the miniaturization of electronic devices, solid state microbatteries are receiving increased attention. Two-dimensional cathodes like

[1] On leave from Institute of Physics, Academia Sinica, P.O. Box 603, Beijing 100080, China.

$LiMn_2O_4$ are particularly important for the thin film batteries. The last part is devoted to the preparation and characterization of thin film of $LiMn_2O_4$, which might be used as a cathode in lithium microbatteries.

2. Influences of sintering temperature

The $LiMn_2O_4$ samples were prepared by solid state reaction. High purity manganese dioxide and lithium carbonate with stoichiometric composition were thoroughly ground and calcined in air in an alumina crucible for 10 h at 450°C, 700°C, 900°C and 1100°C, respectively. Subsequent grinding and sintering were carried out. The samples were characterized by X-ray diffraction using a Siemens D500-B Goniometer with Cu Kα radiation.

It can be seen from X-ray diffraction patterns shown in fig. 1 that the major phase in all the samples is the cubic spinel $LiMn_2O_4$. The sample sintered at 450°C contains Mn_2O_3 and Li_2MnO_3. With increasing sintering temperature the amount of the impurity phases decreased. In the samples sintered at 700°C and beyond only $LiMn_2O_4$ is observed. By careful comparison of the X-ray diffraction line (440) of $LiMn_2O_4$ for various samples as shown in fig. 2 two important differences can be noted:

Firstly, the diffraction lines shift towards lower 2θ values with increase of sintering temperature. Consequently the unit cell is enlarged. A neutron diffraction study has already confirmed an increase from 8.159 Å for a sample sintered at 500°C to 8.196 Å for a sample sintered at 600°C [14]. Secondly, the diffraction line narrows with increasing sintering temperature. Thus at higher temperature it seems that a more perfect cubic spinel phase can be obtained. More recently, similar results have been reported by Mackline et al. [13].

In order to know the effect of sintering temperature on the transport properties, the electrical conductivities of $LiMn_2O_4$ have been measured by ac impedance method using a Solartron 1256 frequency response analyzer over the frequency range 0.1 Hz to 3.5 MHz. The pellets for ac impedance measurement were pressed under a pressure of 1.85 t/cm^2, and sintered in air for 16 h at 1100 and 1200°C, respec-

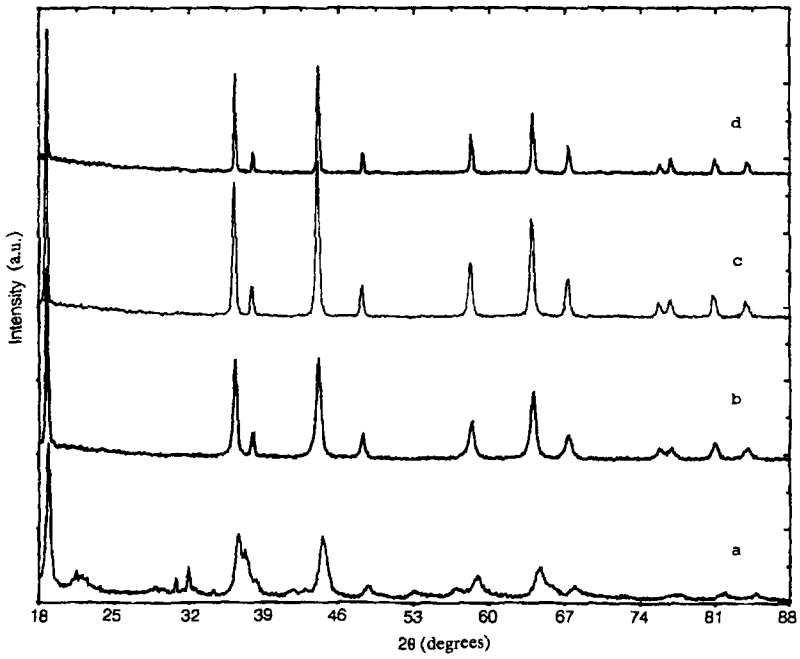

Fig. 1. X-ray diffraction patterns of lithium containing manganese oxides sintered at various temperatures: (a) 450°C, (b) 700°C, (c) 900°C, (d) 1100°C.

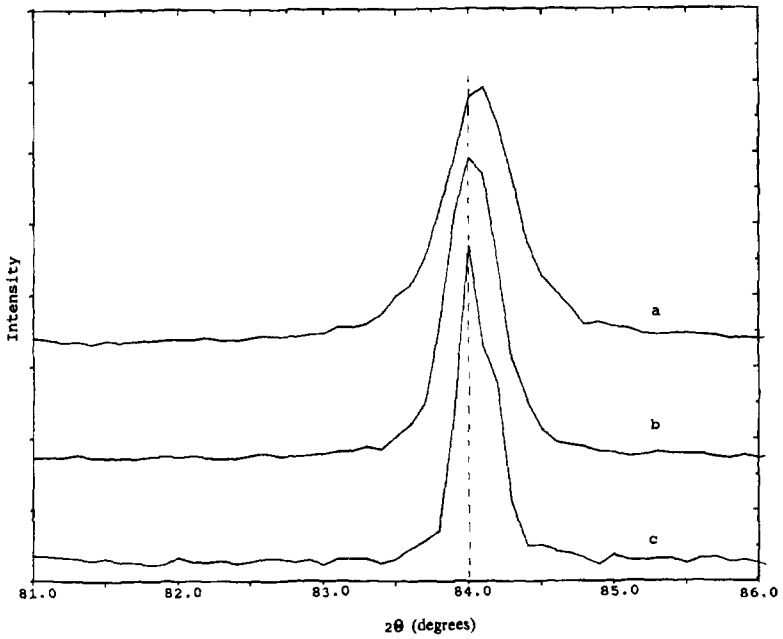

Fig. 2. Comparison of (440) reflection for three samples sintered at: (a) 700°C, (b) 900°C, (c) 1100°C.

tively. The two opposite surfaces were covered with gold as electrodes by dc sputtering using an Edwards sputter coater S150B.

The impedance spectra are composed of two semicircles. The one with higher frequency corresponds to the bulk response, while the lower frequency arc is ascribed to grain boundary polarization phenomena. The conductivity of $LiMn_2O_4$ as a function of temperature is presented in fig. 3. It can be seen that the bulk conductivity of the pellet sintered at 1200°C

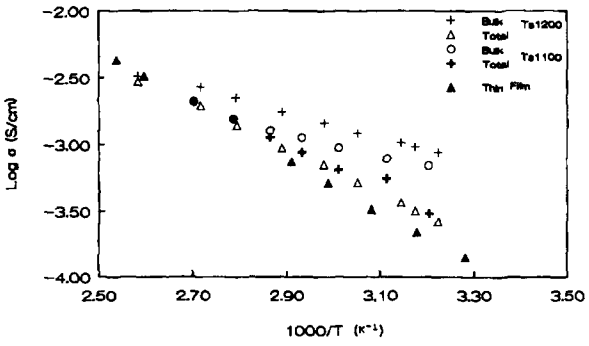

Fig. 3. Electric conductivities of bulk and thin film of $LiMn_2O_4$ as a function of temperature.

is higher than that of the sample sintered at 1100°C. However, the total conductivities of the two samples differ not too much. The activation energies for bulk and total conductivity are 0.20 eV and 0.32 eV, respectively. At this point one might speculate that the samples sintered at higher temperature should have lower grain boundary conductivity. However, considering rather larger difference of activation energy for the grain boundary conduction between the sample sintered at 1200°C, i.e. 0.44 eV, and the sample sintered at 1100°C, i.e. 0.61 eV, it is understandable that samples prepared at higher temperatures still exhibit a higher boundary conductivity at ambient temperature.

It can be concluded from X-ray diffraction and ac impedance study that a higher sintering temperature results in a more pure, more perfect spinel phase, and consequently a higher bulk and grain boundary electrical conductivity. These results do not however, provide any insight into the fact that cathodes sintered at a higher temperature suffer from a large capacity decline within the first 10 cycles, while the samples sintered at 450°C possess good reversibility as reported by Macklin et al. [15]. In order to gain more insight into this difference, the chemical dif-

fusion coefficient for lithium in samples sintered at 450°C and 1100°C has been determined by galvanostatic intermittent titration technique [16]. The values are: $D=4.9\times10^{-9}$ cm^2/s for sample sintered at 450°C; $D=6.0\times10^{-10}$ cm^2/s for sample sintered at 1100°C.

The chemical diffusion coefficient in samples sintered at the lower temperature is obviously higher than that in samples sintered at the higher temperature. This difference may be due to poor crystallization or even impurity phases at the grain boundary of the samples sintered at the lower temperature. This result could explain the difference in reversibility of $LiMn_2O_4$ sintered at various temperatures.

3. Glass formation and electrical conductivity

Samples with various compositions in the system $xLiMn_2O_4$–$(1-x)B_2O_3$ have been prepared. $LiMn_2O_4$, synthesized at 600°C was mixed with high purity H_3BO_3 followed by heating in a platinum crucible in air at 350°C for two hours and subsequently at 1100°C for 15 h. The melt was quenched between two brass blocks. The products varied from amorphous, partially amorphous to crystalline depending on the composition as shown in fig. 4. For $x=0.3$ glassy material can be easily obtained. By improving the heating and quenching conditions glasses with higher concentration of $LiMn_2O_4$ might be obtained, but no attention has yet been payed to this possibility. The glass with composition $0.3LiMn_2O_4$–$0.7B_2O_3$ has been investigated in more detail.

The electrical conductivity of the glass was determined by impedance spectroscopy mentioned above in the temperature range 25–480°C. The samples for conductivity measurement were as-quenched disks without further treatment. The electrodes were silver or gold. The silver electrodes were painted with silver paste followed by baking at 300°C for one hour, while the gold electrodes were prepared by dc sputtering.

The impedance spectra comprise one semicircle through the origin, indicating that the conduction is mainly caused by electronic charge carriers. The electric conductivity of the glass versus inverse tem-

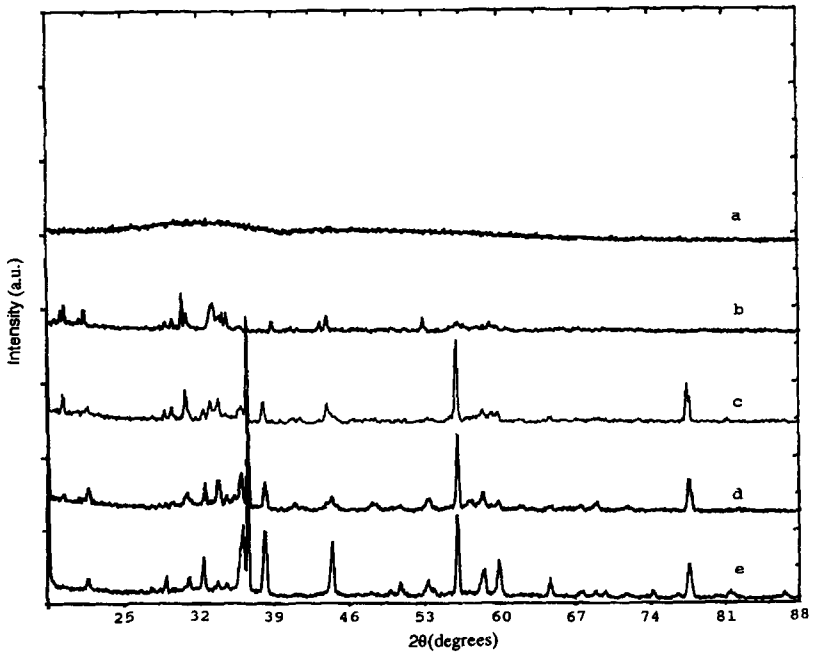

Fig. 4. X-ray diffraction patterns for quenched products from melts with different composition in $xLiMn_2O_4$–$(1-x)B_2O_3$ system: (a) $x=0.3$, (b) $x=0.4$, (c) $x=0.5$, (d) $x=0.6$, (e) $x=0.7$.

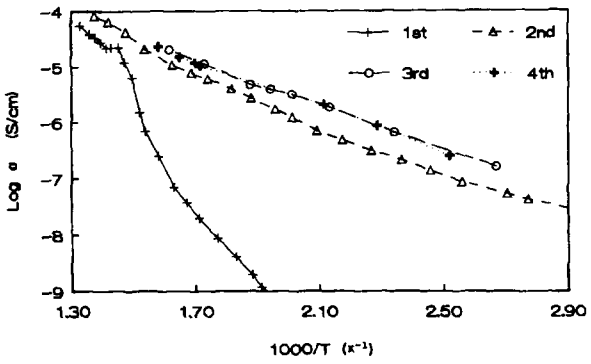

Fig. 5. Conductivity enhancement of glassy $0.3LiMn_2O_4$–$0.7B_2O_3$ during the crystallization process.

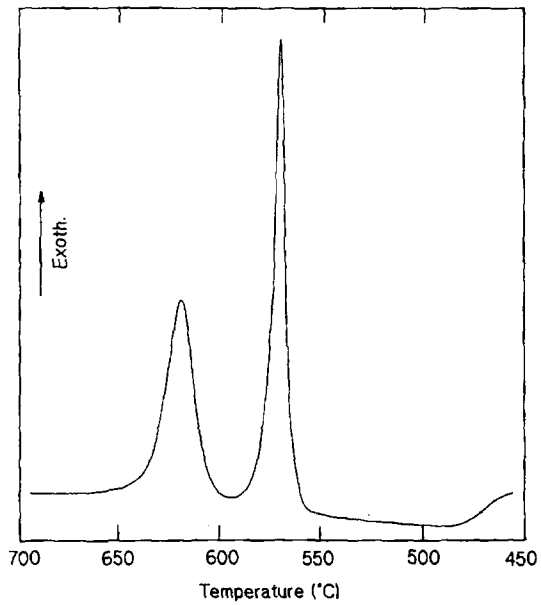

Fig. 6. DTA traces of glassy $0.3LiMn_2O_4$–$0.7B_2O_3$.

perature is shown in fig. 5. Below 340°C the conduction process obeys Arrhenius law, but beyond this temperature the conductivity plot reveals an upward curvature and reaches a maximum at 415°C followed by a slight decrease until 444°C. Then it increases again from 444°C to 480°C. It seems that several processes occur above 340°C. DTA results shown in fig. 6 provide a tool to distinguish these processes. The data in this figure display a glass transition and two crystallization processes. The conductivity enhancement at 340°C is related to the glass transition occurring near 463°C in DTA. The following increase is caused by crystallization appearing at 563°C in DTA. The next sharp increase of conductivity at 440°C is due to the second crystallization process starting around 607°C in DTA. The large discrepancy between the temperatures of these processes as observed in the conductivity measurement and DTA is due to the difference of heating rate, 12°C/min for DTA against 20°C/h for conductivity measurement. After the first run up to 480°C the sample was cooled down to room temperature, and subsequently the conductivity was measured as a function of temperature several times.

By comparing the results obtained in the first and in the second run it is obvious that the crystalline material exhibits a higher conductivity by more than three orders of magnitude. This is the usual case for electronic conductors. Much higher conductivity values in the 3rd run may be related to an incomplete second crystallization process of the glass.

The conductivity enhancement at higher temperature might also be caused by the penetration of silver. In order to exclude this possibility, gold electrodes have been used. The same phenomena were observed. Therefore, the conductivity behaviour described above is ascribed to properties of the glass.

4. Deposition and characterization of thin film

Thin films of $LiMn_2O_4$ were deposited by electron beam evaporation using a four-target Bio Rad apparatus equipped with film thickness monitor. As crucible graphite was used, while as the source material $LiMn_2O_4$ sintered at 1100°C was employed. Stainless steel and glass were used as substrate. The system was pumped to 1×10^{-6} mbar or lower prior to the deposition. The filament current was adjusted to be 7.5 to 8.0 mA, and the acceleration voltage 3.0 to 4.0 kV to maintain the emission current in the range of 15 to 35 mA. The substrate temperature was not controlled and increased from 25 to 200°C. The average deposition rate is 2 to 10 nm/min. The thicknesses of the thin films are between 200 to 700 nm. There has been no extensive investigation to determine whether these conditions yield optimized properties of the $LiMn_2O_4$ thin film.

The thin films are at least mostly crystalline as

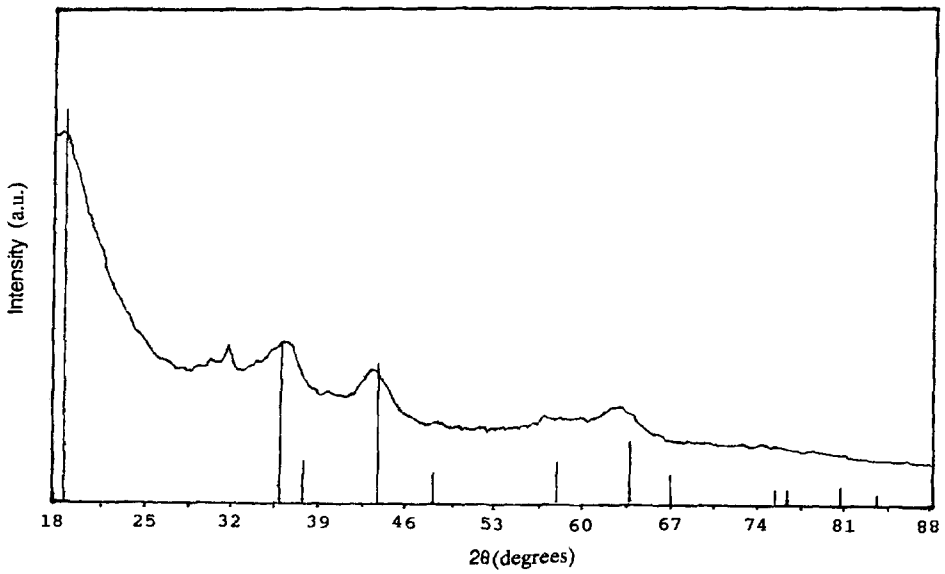

Fig. 7. X-ray diffraction pattern for a thin film of $LiMn_2O_4$.

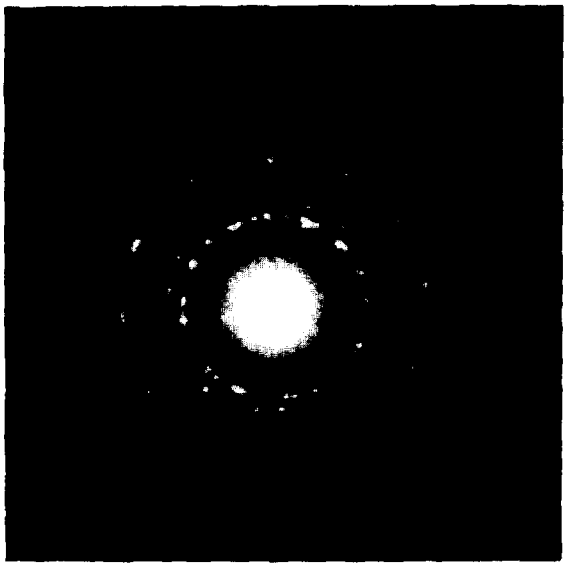

Fig. 8. Electron diffraction pattern for a thin film of $LiMn_2O_4$.

identified by X-ray and electron diffraction (figs. 7 and 8). The standard diffraction lines of $LiMn_2O_4$ are marked in fig. 7 as vertical bars. It can be seen that the diffraction patterns are rather broad with a very strong background. This may be due to a partially amorphous nature of the material, or the result of very fine grains. A TEM image displayed the grain size to be about 10 nm.

The conductivity was measured between 25°C and 130°C with the Van der Pauw method using silver paste as ohmic contacts. The results are also given in fig. 3 along with the data of bulk material for comparison. The conductivity is slightly smaller than the total conductivity of bulk material sintered at 1200°C. Moreover, the activation energy is 0.39 eV which is close to the value of 0.44 eV for grain boundary conduction in sample sintered at 1200°C. This indicates that the grain boundary conduction in the thin films plays an important role.

The chemical diffusion coefficient of lithium has been determined to be 1.3×10^{-14} cm^2/s by the same method as for the bulk. It is four orders of magnitude lower than that of bulk material prepared at 1100°C. This is reasonable. In other systems, such as in InSe the same result has been obtained [17].

A test cell was assembled from a lithium sheet anode, 1M $LiClO_4$ in PC electrolyte, and a $LiMn_2O_4$ thin film. The voltammogram of the cell is shown in fig. 9. The insertion reaction is obvious. The capacity loss within the first 10 cycles is rather large. The discharge curves of such a cell did not show a voltage

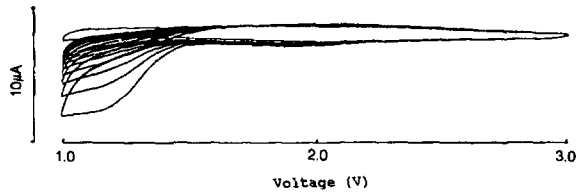

Fig. 9. Cyclic voltammogram of a thin film cell $LiMn_2O_4$/1M $LiClO_4$–PC/Li in the range 1.0–3.0 V at 4 mV/s.

plateau even at a low discharge current density 0.64 $\mu A/cm^2$. No attention has been payed to improve the discharge performances and rechargeability.

Acknowledgement

The authors would like to express their appreciation to Mr. N.M. van der Pers of the Laboratory of Metallurgy for X-ray diffraction Dr. H.W. Zandbergen of the National Centre for High Resolution Electron Microscopy for electron diffraction and HRTEM study. They would like to acknowledge Drs. P.J. Van der Put and Ir. A.V. Zomeren for their encouragement and assistance.

References

[1] J.M. Tarascon and D. Guyomard, J. Electrochem. Soc. 138 (1991) 2864.
[2] M.M. Thackeray, A. de Kock, M.H. Rossouw, D. Liles, R. Bittihn and D. Hoge, J. Electrochem. Soc. 139 (1992) 363.
[3] M.M. Thackeray, W.I.F. David, P.G. Bruce and J.B. Goodenough, Mater. Res. Bull. 18 (1983) 461.
[4] J.C. Hunter, J. Solid State Chem. 39 (1981) 142.
[5] M.M. Thackeray, P.J. Johnson, L.A. De Picciotto, P.G. Bruce and J.B. Goodenough, Mater. Res. Bull. 19 (1984) 179.
[6] A. Mosban, A. Verbaere and M. Tournoux, Mater. Res. Bull. 18 (1983) 1375.
[7] M.M. Thackeray, L.A. De Picciotto, A. De Kock, P.J. Johnson, V.A. Nicholas and K.T. Andendorff, J. Power Sources 21 (1987) 1.
[8] Battery and EV Technol. 12 (1988) 2.
[9] Sony's Lithium Manganese Rechargeable Battery (AA size) (JEC Press Inc., Feb. 1988).
[10] Moli Energy's New Product Data Sheet, JEC Battery Newsletter (1988) p. 15.
[11] T. Nohma, Y. Yamamoto, K. Nishio, I. Nakane and N. Furukawa, J. Power Sources 32 (1990) 373.
[12] F. Lubin, A. Lecerf, M. Broussely and J. Labat, J. Power Sources 34 (1991) 161.
[13] M. Uchiyama, S. Slane, E. Plichta and M. Salomon, J. Electrochem. Soc. 136 (1989) 36.
[14] M.H. Rossouw, A. Dekock, L.A. De Picciotto, M.M. Thackeray, W.I.F. David and R.M. Ebberson, Mater. Res. Bull. 25 (1990) 173.
[15] W.J. Macklin, R.J. Neat and R.J. Powell, J. Power Sources 34 (1991) 39.
[16] W. Weppner and R.A. Huggins, J. Electrochem. Soc. 124 (1977) 1569.
[17] C. Julien, I. Samaras, M. Tsakiri, P. Dzwonkowski and M. Balkanski, Mater. Sci. Eng. B 3 (1989) 25.